ADAPTIVE CONTROL BASED FLYING QUALITY DESIGN FOR HELICOPTERS

Wu Wei
Nanjing University of Aeronautics and Astronautics, Nanjing, China

Abstract

A comprehensive flight control law design method based on adaptive control is presented in this paper. The proposed method consists of three basic modules – model decoupling, online system identification and adaptive pole placement. The model decoupling module decouples the helicopter flight dynamics model based on dynamic inversion technique. This procedure helps to reduce the difficulties in online system identification and adaptive control design. In online system identification module, a recursive extended least squares algorithm is established to identify the augmented linear flight dynamics model which is composed of helicopter model and unideal noise model. The helicopter model parameters and the noise parameters are identified simultaneously which improves the identification accuracy as well as robustness compared with conventional method. Pole placement is implemented in the last module to make a helicopter keep tracking the idea poles which can be designed according to ADS-33E-PRF. The adaptive rule in this step is designed based on eigenvalue analysis of the model to remove all unnecessary oscillations of the control parameters. An adaptive controller is designed according to the developed method for the UH-60 helicopter based on a nonlinear simulation program. Typical response types are also implemented. The simulation results show that the designed adaptive controller has high performance as well as robustness in both hover and forward flight.

1. INTRODUCTION

The helicopter is a special aircraft which can perform hovering, vertical takeoff and landing as well as low speed maneuvers, and it has already been widely used in civil and military domain. However, the flying quality of a helicopter is poor due to many reasons, such as a helicopter is highly coupled, it is quite unstable and the vibration and noise level of a helicopter is high etc. The poor flying quality brings many problems in actual flight, for example, the pilot need to make compensation controls to eliminate undesirable cross coupling responses at any time during the flight which means the workload is very high. Moreover, in some severe condition, such as during aggressive maneuver procedure, the poor flying quality will cause safety problems. Therefore, the operational capability and the mission effectiveness of a helicopter are limited for these reasons. In order to solve these problems, the flying quality of a helicopter must be improved. A proper flying quality specification is required for flying quality design. However, since the dynamic characteristics of a helicopter are very complex, the helicopter flying quality specification is also experienced a long time of evolution [1]. In the first helicopter flying quality specification, the MIL-H-8501 and its revised version (the MIL-H-8501A), the primary requirements only consisted of simple time domain parameters. However, in the current specification, the ADS-33E-PRF [2], the coverage of design requirements is expanded significantly. When we have the specification on hand, the rest problem is how to improve the flying quality of a helicopter based on certain specification. Basically, there are two different ways to deal with this problem. The first way is to optimize some of the design parameters of a helicopter such as rotor diameter, rotor height, rotor flapping hinge offset, position and area of vertical tail or horizontal tail etc. However, since the helicopter is highly coupled and the dynamic behavior of a helicopter is very complex, adjusts one certain design parameter may increase the flying quality level of some requirements defined in the specification but decrease the others. Therefore, the optimization results of all design parameters will always be a compromised solution. The second way is to design a proper flight control system with high performance, and it has already been proven that this kind of approach is much more efficient and effective than the first way.

However, the complexity of a helicopter also brings many difficulties in flight control system design [3-4]. Although most of the current controllers used in helicopters are designed based on classical PID control method, the disadvantages of PID controllers in helicopter flight control are also very obvious. For example, a helicopter has strong nonlinearity, which means the dynamic characteristics of a helicopter have large differences

in different flight states. If a PID controller is designed in one flight state, such as hover, the performance of the controller will be decreased quite a lot in other flight states, forward flight for instance. Therefore, the overall performance of a PID controller is limited. In order to overcome the shortages of PID controllers, there are a lot of researches concentrate on development of advanced flight control design tools based on modern control theory. Optimal control and model-following control method have already been used to design the flight control laws for helicopters that equipped with fly-by-wire or flight-by-light control system for decades [5-7]. Flight test results indicate the performance of such controllers is increased significantly compared with PID controllers. Robust control is another advanced tool for helicopter flight control law design [8-9]. In this kind of method, the influences of model uncertainties caused by nonlinearity, measurement noise and environment disturbances etc. are considered during the design process, so the controllers designed by this approach will be much more robust than PID controllers. Adaptive control, which is even more powerful than robust control, is a perfect tool for flight control law design of complex aircraft including helicopters. There are plenty of papers addressed their achievements in adaptive control research, and these studies proposed many excellent ideas in neural adaptive control and model reference adaptive control for fixed wings and helicopters [10-16]. New theoretical achievements for adaptive control design were also obtained in recent years [17]. However, it is still a challenge of designing a stable adaptive controller with instant control accuracy at different flight states for a helicopter today due to its complicated dynamic characteristics.

A comprehensive adaptive control design method is developed in this paper for improving flying quality of a helicopter. The flight control law is designed using combined adaptive and dynamic inversion technique. An improved online system identification algorithm is also established that is able to consider the influence of measurement noise. The adaptive strategy is selected to ensure the controller keeps high performance from hover to maximum forward flight speed, while the feedback coefficients have minimum changing frequency. Application of the developed method to a UH-60 helicopter shows the proposed adaptive control design method is effective, efficient and robust.

2. GENERAL DESCRIPTION OF THE DESIGN METHOD

A general controller structure based on the developed design method can be found in Fig. 1. Basically, there are two control loops in the controller. The inner loop is used to decouple the helicopter, and the outer loop is designed to make the helicopter reach required flying quality level according to the ADS-33E-PRF. Since the identification of full coupled flight dynamics model is a difficult task especially in real time, the helicopter is decoupled before the identification module to simplify the identification problem by a dynamic inversion controller. Then in the system identification module, only several decoupled or weak coupled models are need to be identified. In the pole placement controller module, ideal poles in each control channel are designed for different purpose according to the ADS-33E-PRF, and a pole placement algorithm is applied to the identified flight dynamics model to ensure the poles of final closed-loop model are identical to ideal poles. Because the sampling frequency of airborne sensors is high, so the differences among each identified models in contiguous sampling points are very small. In some cases, such as in steady hover or steady forward flight, the identified models are nearly identical all the time. Therefore, there is no need to do pole placement at each sampling points. The adaptive rule is set then based on model analysis to avoid unnecessary calculation of feedback matrix. As a consequence, the efficiency and the stability of the controller are increased.

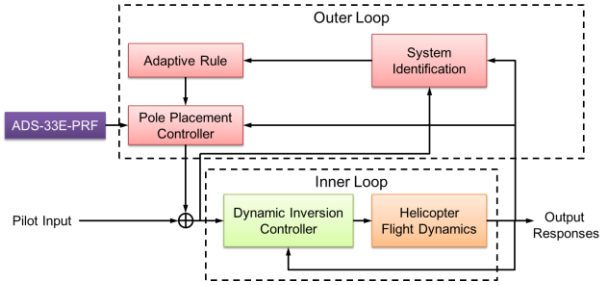

Figure 1: General Structure of the Adaptive Controller.

Details of the three basic modules, i.e. inner loop decoupling controller, online system identification and adaptive pole placement will be discussed in the following sections. A nonlinear model of UH-60 helicopter which can be found in Ref. [23] is used in this paper to do numerical simulation and validation of the designed adaptive controller.

3. INNER LOOP DECOUPLING CONTROLLER

In order to decouple a helicopter, an inner loop controller is designed based on dynamic inversion technique. Because the helicopter flight dynamics in Fig. 1 is nonlinear, so a nonlinear dynamic inversion solver is the best tool to deal with this problem. However, since the structure of helicopter flight dynamics model is very complex, the nonlinear dynamic inversion problem of a helicopter is also very complicated. Besides, the nonlinear dynamic inversion calculation is very time consuming, it is difficult to use such solver in real time. Therefore, a linear dynamic inversion solver is applied in this paper, while a linear state space flight dynamics model is used in dynamic inversion calculation.

Fig. 2 shows the basic principle of dynamic inversion controller. A linear state space flight dynamics model of a helicopter is represented as Eq. (1). The feedback matrix $\boldsymbol{K}_{inv}$ and feedforward matrix $\boldsymbol{L}_{inv}$ can be determined according to current stability matrix $\boldsymbol{A}$ and control matrix $\boldsymbol{B}$ of a helicopter.

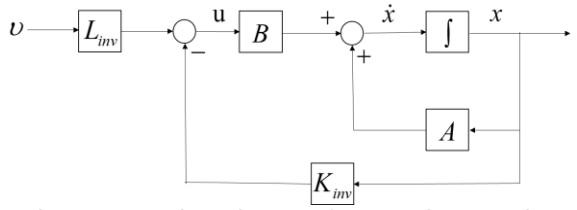

Figure 2: Basic Scheme of Dynamic Inversion Controller.

$$\dot{\boldsymbol{x}} = \boldsymbol{A}\boldsymbol{x} + \boldsymbol{B}\boldsymbol{u} \tag{1}$$

A closed-loop model is easily obtained according to Fig.2, which can be written as Eq. (2). It is obviously that the closed-loop model can be decoupled by selecting proper $\boldsymbol{K}_{inv}$ and $\boldsymbol{L}_{inv}$ matrix. In order to obtain the solution, matrix inverse calculation is required. However, the control matrix $\boldsymbol{B}$ is not a square matrix, which means the normal inverse matrix does not exist.

$$\dot{\boldsymbol{x}} = (\boldsymbol{A} - \boldsymbol{B}\boldsymbol{K}_{inv})\boldsymbol{x} + \boldsymbol{B}\boldsymbol{L}_{inv}\boldsymbol{\upsilon} \tag{2}$$

Considering there are both fast and slow state variables in $\boldsymbol{x}$, the whole system will be stable if the fast state is stabilized. Therefore, Eq. (2) can be replaced by Eq. (3) for solving the dynamic inversion problem.

$$\dot{\boldsymbol{x}}_{inv} = (\boldsymbol{A}_{inv} - \boldsymbol{B}_{inv}\boldsymbol{K}_{inv})\boldsymbol{x} + \boldsymbol{B}_{inv}\boldsymbol{L}_{inv}\boldsymbol{\upsilon} \tag{3}$$

In which, $\boldsymbol{x}_{inv} = [w, p, q, r]^T$,

$\boldsymbol{x} = [u, v, w, p, q, r, \phi, \theta, \psi]^T$,

$\boldsymbol{\upsilon} = \left[\delta_{long}, \delta_{lat}, \delta_{col}, \delta_{ped}\right]^T$, $\boldsymbol{A}_{inv}$ is a 4×9 matrix, $\boldsymbol{B}_{inv}$ is a 4×4 matrix

The next step is to define ideal decoupled model structure. Weak decoupled stability matrix $\boldsymbol{A}_{\exp}$ and control matrix $\boldsymbol{B}_{\exp}$ are shown in Eq. (4) and Eq. (5) respectively. The reason for not using fully decoupled model is to keep lateral-directional oscillation modes in the model. In ADS-33E-PRF, special requirements are defined for these modes such as Dutch roll. Therefore, these modes should be remained and optimized in pole placement module.

$$\boldsymbol{A}_{\exp} = \begin{bmatrix} 0 & 0 & Z_w & 0 & 0 & 0 & 0 & 0 & 0 \\ 0 & 0 & 0 & L_p & 0 & L_r & 0 & 0 & 0 \\ 0 & 0 & 0 & 0 & M_q & 0 & 0 & 0 & 0 \\ 0 & 0 & 0 & N_p & 0 & N_r & 0 & 0 & 0 \end{bmatrix} \tag{4}$$

$$\boldsymbol{B}_{\exp} = \begin{bmatrix} 0 & 0 & Z_{\delta_{col}} & 0 \\ 0 & L_{\delta_{lat}} & 0 & L_{\delta_{ped}} \\ M_{\delta_{long}} & 0 & 0 & 0 \\ 0 & N_{\delta_{lat}} & 0 & N_{\delta_{ped}} \end{bmatrix} \tag{5}$$

The solution for $\boldsymbol{K}_{inv}$ and $\boldsymbol{L}_{inv}$ matrix can be easily obtained by combing Eq. (3), Eq. (4) and Eq. (5), as shown in Eq. (6) and Eq. (7).

$$\boldsymbol{L}_{inv} = \boldsymbol{B}_{inv}^{-1}\boldsymbol{B}_{\exp} \tag{6}$$

$$\boldsymbol{K}_{inv} = (\boldsymbol{A}_{inv} - \boldsymbol{A}_{\exp})\boldsymbol{B}_{inv}^{-1} \tag{7}$$

A decoupling controller is designed for a UH-60 helicopter in hover condition based on the preceding method. The solution can be found in Eq. (8) and Eq. (9).

$$\boldsymbol{L}_{inv} = \begin{bmatrix} 0.9993 & 0.0106 & 0.0218 & -0.0443 \\ -0.0337 & 0.997 & 0.0422 & 0.0046 \\ -0.0172 & 0 & 0.9919 & 0.0733 \\ 0.0015 & 0 & -0.1055 & 0.9922 \end{bmatrix} \tag{8}$$

$$\boldsymbol{K}_{inv} = \begin{bmatrix} 0.0105 & 0.0394 & 0.0062 & 0.9375 & -0.0014 & -0.0092 & -0.0036 & 0.0078 & 0 \\ 0.0073 & -0.0214 & 0.0015 & -0.0315 & -2.0038 & 0.0019 & -0.0070 & 0.0151 & 0 \\ -0.0028 & 0.0017 & 0 & -0.0149 & -0.0804 & 0.0377 & -0.1638 & 0.3542 & 0 \\ 0.0035 & 0.0169 & -0.0033 & 0.0012 & -0.4632 & -0.0040 & 0.0174 & -0.0377 & 0 \end{bmatrix} \tag{9}$$

Step inputs of longitudinal cyclic, lateral cyclic, collective and pedal are applied to the decoupled model respectively. Simulation results are shown in Fig. 3 ~ Fig. 6. It is obviously to see that the longitudinal channel and vertical channel are fully decoupled, while the lateral channel and directional channel are weakly coupled. Moreover, the performance of the controller is kept well with flight states changing.

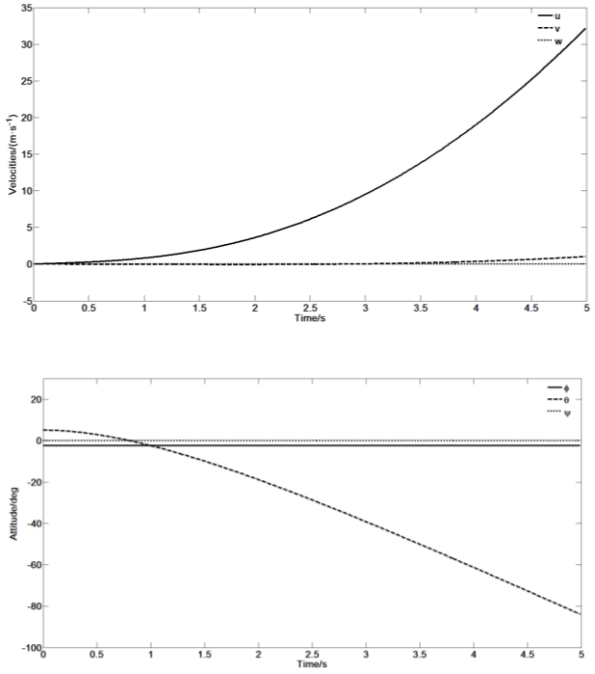

Figure 3: Decoupled Helicopter Responses with Longitudinal Cyclic Step Input.

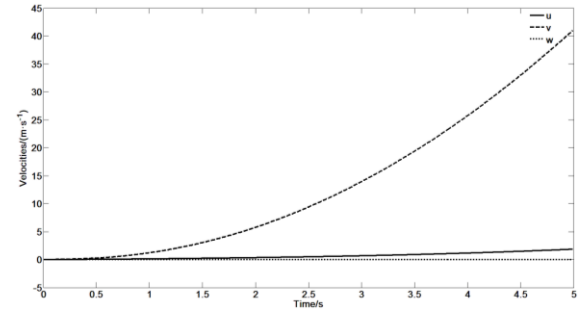

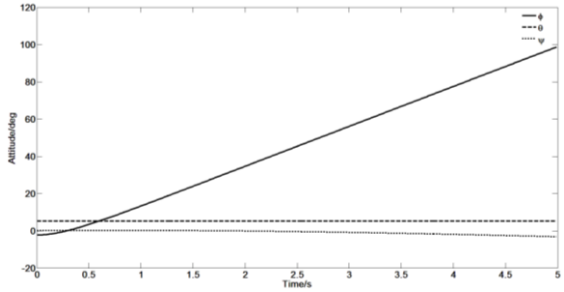

Figure 4: Decoupled Helicopter Responses with Lateral Cyclic Step Input.

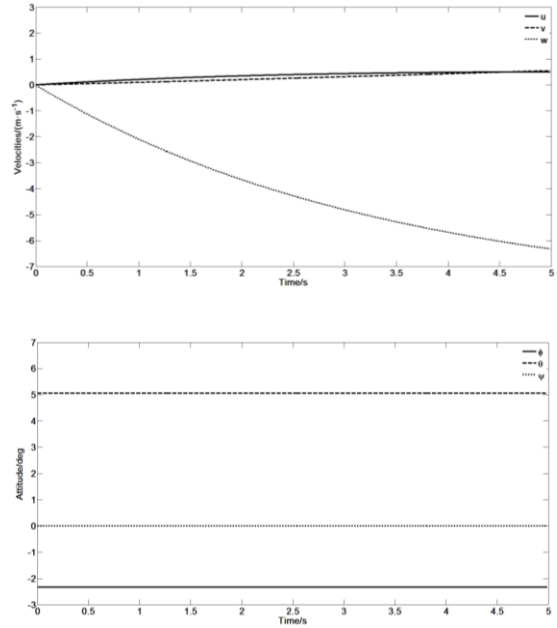

Figure 5: Decoupled Helicopter Responses with Collective Step Input.

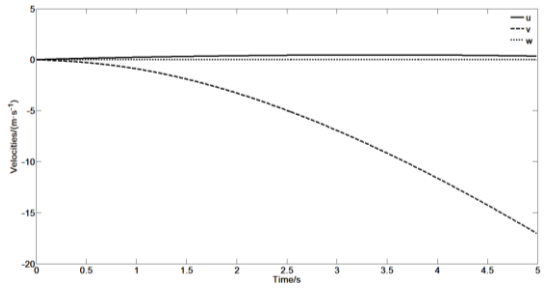

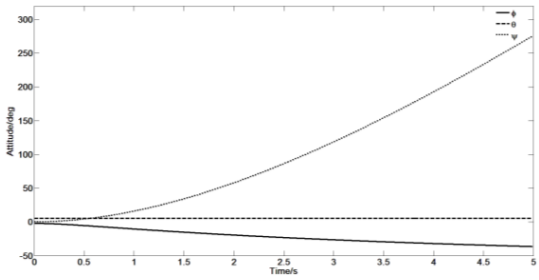

Figure 5: Decoupled Helicopter Responses with Collective Step Input.

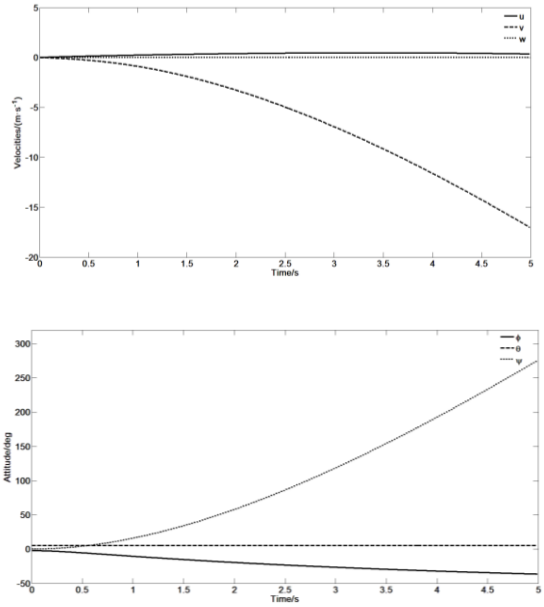

Figure 6: Decoupled Helicopter Responses with Pedal Step Input.

4. ONLINE SYSTEM IDENTIFICATION

Online system identification is a very important module in adaptive controller, since the accuracy of identified model has large influences on controller's performance. However, the identification problem of a helicopter is very complex. Nearly 5 decades have been past from the first attempt in applying system identification into helicopter flight dynamics modeling, and plenty of methods have been developed both in time domain and frequency domain [18-22]. However, most of these methods are used for offline identification purpose, and it is not possible to integrate these comprehensive methods into an adaptive controller. The most frequently used identification algorithm in an adaptive controller currently is recursive least squares (RLS) method. This kind of method is easy to implement and efficient, but it is not robust to noise. A helicopter has high level of vibration and measurement noise during the flight, which means the measured responses are contaminated. Although there are low pass filters in flight control system, the influences of measurement noise to measured data are still existed. Theoretically speaking, the least squares estimator is unbiased and consistent only when there is white noise or no noise in measured data. Therefore, in most of the current online identification methods, measurement noise is neglected or simplified to white noise. But unfortunately, the measurement noise of a helicopter will always be colored, and the white noise assumption will bring additional identification errors.

In this paper, a recursive extended least squares algorithm is established. Because the helicopter is decoupled before identification, full coupled flight dynamics model identification problem can be replaced by identifying 3 decoupled and weak coupled models, as shown in Eq. (10) ~ Eq. (12).

$$\begin{bmatrix}\dot{u}\\ \dot{q}\\ \dot{\theta}\end{bmatrix}=\begin{bmatrix}X_u & X_q & -g\cos\theta_0\\ M_u & M_q & 0\\ 0 & 1 & 0\end{bmatrix}\begin{bmatrix}u\\ q\\ \theta\end{bmatrix}+\begin{bmatrix}X_{\delta_{long}}\\ M_{\delta_{long}}\\ 0\end{bmatrix}\delta_{long} \tag{10}$$

$$\dot{w}=Z_w\cdot w+Z_{\delta_{col}}\cdot\delta_{col} \tag{11}$$

$$\begin{bmatrix}\dot{v}\\ \dot{p}\\ \dot{r}\\ \dot{\phi}\\ \dot{\psi}\end{bmatrix}=\begin{bmatrix}Y_v & Y_p+w_0 & Y_r-u_0 & g\cos\theta_0\cos\phi_0 & 0\\ L_v & L_p & L_r & 0 & 0\\ N_v & N_p & N_r & 0 & 0\\ 0 & 1 & \tan\theta_0 & 0 & 0\\ 0 & 0 & 1/\cos\theta_0 & 0 & 0\end{bmatrix}\begin{bmatrix}v\\ p\\ r\\ \phi\\ \psi\end{bmatrix}+\begin{bmatrix}Y_{\delta_{lat}} & Y_{\delta_{ped}}\\ L_{\delta_{lat}} & L_{\delta_{ped}}\\ N_{\delta_{lat}} & N_{\delta_{ped}}\\ 0 & 0\\ 0 & 0\end{bmatrix}\begin{bmatrix}\delta_{lat}\\ \delta_{ped}\end{bmatrix} \tag{12}$$

In order to consider the influences of unideal measurement noise, a second order noise model is established as shown in Eq. (13).

$$\boldsymbol{e}(t)=\boldsymbol{\xi}(t)+\boldsymbol{d}_1\boldsymbol{\xi}(t-\Delta t)+\boldsymbol{d}_2\boldsymbol{\xi}(t-2\Delta t) \tag{13}$$

In which, $\boldsymbol{e}$ is unideal noise vector, t is time variable, Δt is sampling time interval, $\boldsymbol{d}_1$ and $\boldsymbol{d}_2$ are noise model parameters vector, $\boldsymbol{\xi}$ is noise description vector which can be approximated by model prediction error.

Substitutes Eq. (13) into Eq. (10) ~ Eq. (12), and after some mathematical manipulation, a standard discrete least squares identification model can be obtained as shown in Eq. (14). Detailed structure of each component in Eq. (14) can be found in Eq. (15) ~ Eq. (17) for different models.

$$\boldsymbol{y}(k)=\boldsymbol{h}^T(k)\boldsymbol{\theta}+\bar{\boldsymbol{e}}(k) \tag{14}$$

Longitudinal model:

$$\begin{cases} \boldsymbol{y}^{long}(k)=\left[a_x(k),\dot{q}(k)\right]^T \\ \boldsymbol{\theta}^{long}=\left[X_u,X_q,X_{\delta_{long}},d_1^{long1},d_2^{long1},M_u,M_q,M_{\delta_e},d_1^{long2},d_2^{long2}\right]^T \\ \boldsymbol{h}^{long}(k)=\begin{bmatrix} u(k) & q(k) & \delta_{long}(k) & \xi_1^{long}(k-1) & \xi_1^{long}(k-2) & 0 & 0 & 0 & 0 & 0 \\ 0 & 0 & 0 & 0 & 0 & u(k) & q(k) & \delta_{long}(k) & \xi_2^{long}(k-1) & \xi_2^{long}(k-2) \end{bmatrix}^T \\ \overline{\boldsymbol{e}}^{long}(k)=\left[\xi_1^{long}(k),\xi_2^{long}(k)\right]^T \end{cases} \tag{15}$$

Vertical model:

$$\begin{cases} \boldsymbol{y}^{ver}(k)=\left[a_z(k)\right]^T \\ \boldsymbol{\theta}^{ver}=\left[Z_w,Z_{\delta_{col}},d_1^{ver},d_2^{ver}\right]^T \\ \boldsymbol{h}^{ver}(k)=\left[w(k)\quad \delta_{col}(k)\quad \xi_1^{ver}(k-1)\quad \xi_1^{ver}(k-2)\right]^T \\ \overline{e}^{ver}(k)=\xi_1^{ver}(k) \end{cases} \tag{16}$$

Lateral-directional model:

$$\begin{cases} \boldsymbol{y}^{latyaw}(k)=\left[a_y(k),\dot{p}(k),\dot{r}(k)\right]^T \\ \boldsymbol{\theta}^{latyaw}=\left[Y_v,Y_p,Y_r,Y_{\delta_{lat}},Y_{\delta_{ped}},d_1^{latyaw1},d_2^{latyaw1},L_v,L_p,L_r,L_{\delta_{lat}},L_{\delta_{ped}},d_1^{latyaw2},d_2^{latyaw2},N_v,N_p,N_r,N_{\delta_{lat}},N_{\delta_{ped}},d_1^{latyaw3},d_2^{latyaw3}\right]^T \\ \boldsymbol{h}^{latyaw}=\begin{bmatrix} v(k) & p(k) & r(k) & \delta_{lat}(k) & \delta_{ped}(k) & \xi_1^{latyaw}(k-1) & \xi_1^{latyaw}(k-2) & 0 & 0 & 0 & 0 & 0 & 0 & 0 \\ 0 & 0 & 0 & 0 & 0 & 0 & 0 & v(k) & p(k) & r(k) & \delta_{lat}(k) & \delta_{ped}(k) & \xi_2^{latyaw}(k-1) & \xi_2^{latyaw}(k-2) \\ 0 & 0 & 0 & 0 & 0 & 0 & 0 & 0 & 0 & 0 & 0 & 0 & 0 & 0 \end{bmatrix} \\ \qquad\qquad \begin{bmatrix} 0 & 0 & 0 & 0 & 0 & 0 & 0 \\ 0 & 0 & 0 & 0 & 0 & 0 & 0 \\ v(k) & p(k) & r(k) & \delta_{lat}(k) & \delta_{ped}(k) & \xi_3^{latyaw}(k-1) & \xi_3^{latyaw}(k-2) \end{bmatrix}^T \\ \overline{\boldsymbol{e}}^{latyaw}(k)=\left[\xi_1^{latyaw}(k),\xi_2^{latyaw}(k),\xi_3^{latyaw}(k)\right]^T \end{cases} \tag{17}$$

Standard recursive least squares iterations, as shown in Eq. (18), can be applied directly to the above extended models. Data saturation problem is avoided by adding a window with length *L* in the identification process, when the number of data used in identification reaches *L*, the covariance matrix ***P*** will be reset according to current states.

$$\begin{cases} \hat{\boldsymbol{\theta}}(k)=\hat{\boldsymbol{\theta}}(k-1)+\boldsymbol{K}(k)[\boldsymbol{y}(k)-\boldsymbol{h}^T(k)\hat{\boldsymbol{\theta}}(k-1)] \\ \boldsymbol{K}(k)=\boldsymbol{P}(k-1)\boldsymbol{h}(k)\left[\boldsymbol{h}^T(k)\boldsymbol{P}(k-1)\boldsymbol{h}(k)+1\right]^{-1} \\ \boldsymbol{P}(k)=\left[\boldsymbol{I}(k)-\boldsymbol{K}(k)\boldsymbol{h}^T(k)\right]\boldsymbol{P}(k-1) \end{cases} \tag{18}$$

Identification results of a UH-60 helicopter in hover condition are shown in Table1 ~ Table 3 and Fig. 7 ~ Fig. 8, while comparative study between the developed method in this paper with standard RLS algorithm is also conducted. 3-2-1-1 input signal, which is different with sweep excitation used in identification procedure, is applied to verify the identified models. The verification results are shown in Fig. 9 ~ Fig. 12. It is apparently that the identification accuracy of the developed method is increased significantly compared with standard RLS method, and this is especially true when the signal to noise ratio is low (Fig. 11 and Fig. 12). This is because in standard RLS algorithm, noise is treated as white random signal which has zero mean value and constant variance. However, the real noise is colored that has non-zero mean value and time variant variance. So there exists a bias term between the ideal noise and the real noise, and biased estimation of model parameters is obtained. In the method developed in this paper, the bias term is represented as colored noise model. Therefore the bias in helicopter model parameter identification

is eliminated. Fig. 13 shows the noise prediction error, and good prediction capability of the noise model is proven.

Model Parameter	Identified in This Paper	Identified by Standard RLS	True Value
X_u	-0.0236	-0.0265	-0.02349
X_q	2.8395	2.8827	2.809
$X_{\delta_{long}}$	-1.6589	-1.6347	-1.659
d_1^{long1}	0.4870	-	0.5
d_2^{long1}	0.1662	-	0.2
M_u	0.0036	0.0038	0.003554
M_q	-0.8199	-0.8996	-0.8161
$M_{\delta_{long}}$	0.3348	0.3219	0.3346
d_1^{long2}	0.4996	-	0.5
d_2^{long2}	0.2433	-	0.2

Table1: Identification Results of Longitudinal Model.

Model Parameter	Identified in This Paper	Identified by Standard RLS	True Value
Z_w	-0.2923	-0.2804	-0.2931
$Z_{\delta_{col}}$	-7.9217	-7.8761	-7.921
d_1^{ver1}	0.5211	-	0.5
d_2^{ver1}	0.1985	-	0.2

Table 2: Identification Results of Vertical Model.

Model Parameter	Identified in This Paper	Identified by Standard RLS	True Value
Y_v	-0.0474	-0.0501	-0.0473
Y_p	-1.7377	-1.8916	-1.723
Y_r	0.6428	0.6806	0.6383
$Y_{\delta_{lat}}$	0.9384	0.7833	0.942
$Y_{\delta_{ped}}$	-1.4885	-1.4674	-1.486
$d_1^{latyaw1}$	0.5197	-	0.5
$d_2^{latyaw1}$	0.2239	-	0.2
L_v	-0.0415	-0.04874	-0.04124
L_p	-3.5429	-3.5992	-3.551
L_r	0.0807	0.0560	0.07467
$L_{\delta_{lat}}$	1.3243	1.2362	1.334
$L_{\delta_{ped}}$	-0.8341	-0.8043	-0.8406
$d_1^{latyaw2}$	0.5321	-	0.5
$d_2^{latyaw2}$	0.2434	-	0.2
N_v	0.0096	0.0100	0.00976
N_p	-0.0981	-0.1295	-0.1013
N_r	-0.3312	-0.3596	-0.3342
$N_{\delta_{lat}}$	0.0259	0.0371	0.02734
$N_{\delta_{ped}}$	0.6042	0.6507	0.604
$d_1^{latyaw3}$	0.4997	-	0.5
$d_2^{latyaw3}$	0.1910	-	0.2

Table 3: Identification Results of Lateral-directional Model.

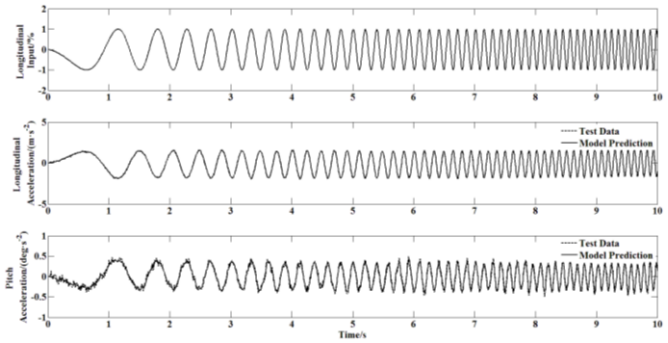

Figure 7: Longitudinal decoupled model identification result.

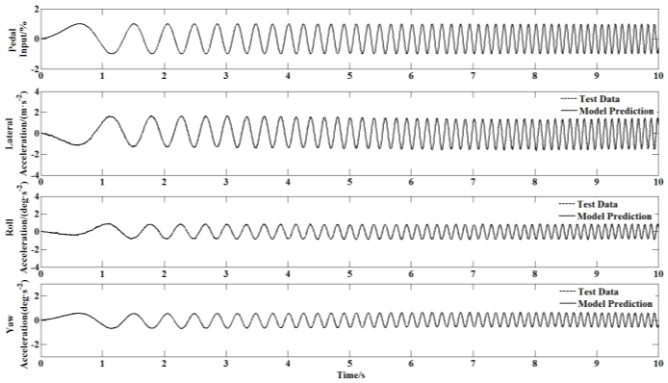

Figure 8: Lateral-directional weak coupled model identification result.

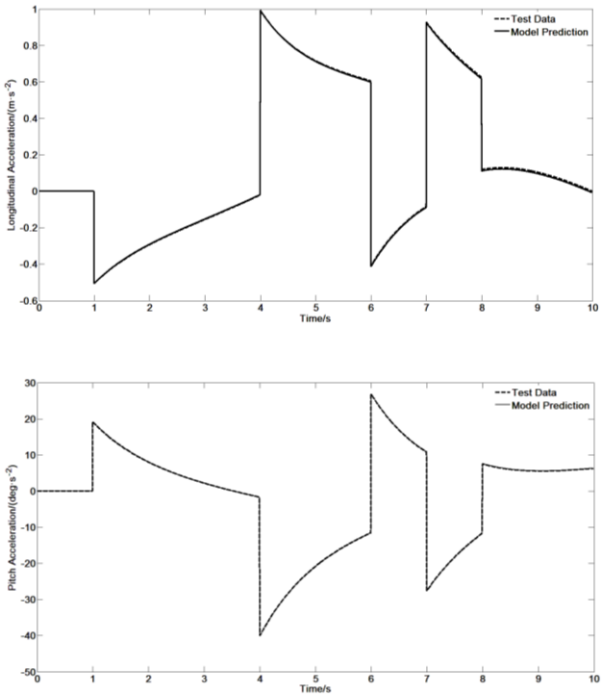

Figure 9: Verification of Longitudinal Model without Noise Contamination.

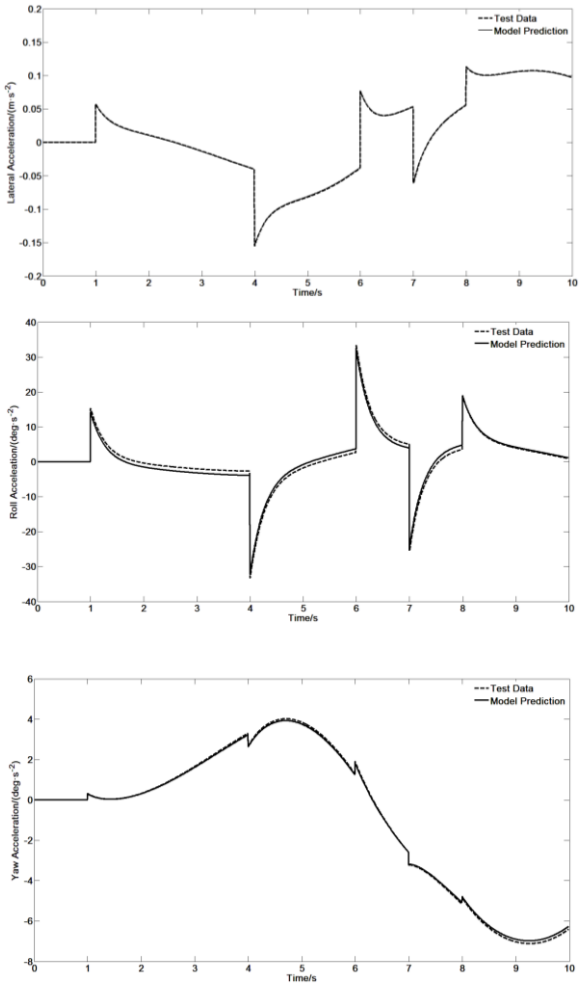

Figure 10: Verification of Lateral-directional Model without Noise Contamination.

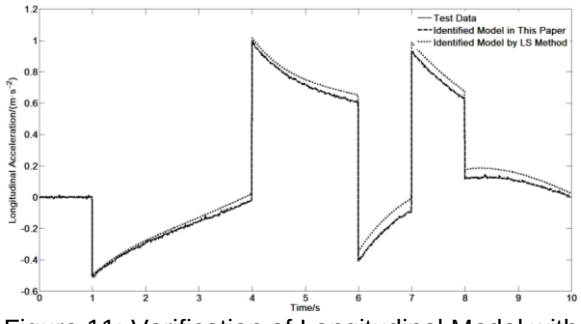

Figure 11: Verification of Longitudinal Model with Colored Noise Contamination.

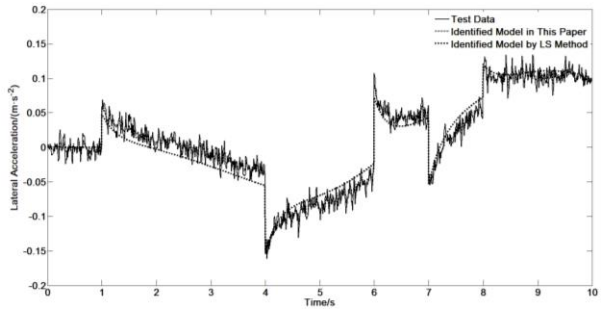

Figure 12: Verification of Lateral-directional Model with Colored Noise Contamination.

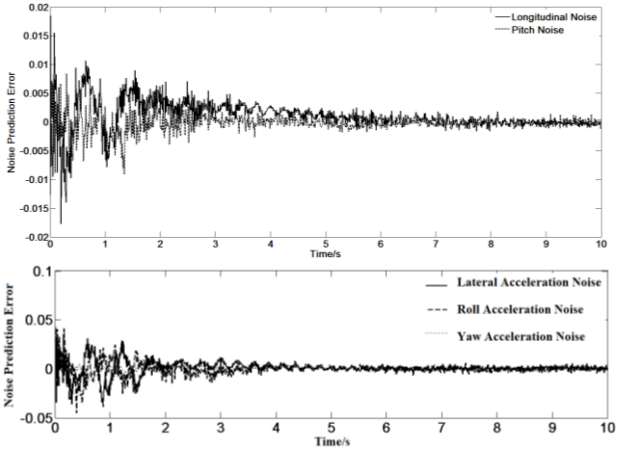

Figure 13: Verification of Colored Noise Model.

5. ADAPTIVE POLE PLACEMENT

Pole placement is a powerful tool in modern control theory, and it is very suitable for flying quality design. This is because in ADS-33E-PRF, many of the flying quality requirements can be represented by poles or eigenvalues. Therefore, it is very convenient to use ideal poles or eigenvalues to implement flying quality design. If the closed loop model of a helicopter has the designed poles or eigenvalues, then this helicopter will reach the expected flying quality level. Since different requirements are defined for hover/low speed flight and forward flight in ADS-33E-PRF, ideal poles should also be designed separately in different flight states.

The flight dynamics model used in adaptive pole placement is 6 degrees of freedom state space model, the same as Eq. (1). However, since the model is decoupled, stability matrix A and control matrix B in Eq. (1) now have very simple structure, as shown in Eq. (19) and Eq. (20).

$$\boldsymbol{A}=\begin{bmatrix} X_u & 0 & 0 & 0 & X_q & 0 & 0 & -g\cos\theta_0 & 0 \\ 0 & Y_v & 0 & Y_p & 0 & Y_r & g\cos\theta_0\cos\phi_0 & 0 & 0 \\ 0 & 0 & Z_w & 0 & 0 & 0 & 0 & 0 & 0 \\ 0 & L_v & 0 & L_p & 0 & L_r & 0 & 0 & 0 \\ M_u & 0 & 0 & 0 & M_q & 0 & 0 & 0 & 0 \\ 0 & N_v & 0 & N_p & 0 & N_r & 0 & 0 & 0 \\ 0 & 0 & 0 & 1 & 0 & \tan\theta_0 & 0 & 0 & 0 \\ 0 & 0 & 0 & 0 & 1 & 0 & 0 & 0 & 0 \\ 0 & 0 & 0 & 0 & 0 & 1/\cos\theta_0 & 0 & 0 & 0 \end{bmatrix} \quad (19)$$

$$\boldsymbol{B}=\begin{bmatrix} X_{\delta_{long}} & 0 & 0 & 0 \\ 0 & Y_{\delta_{lat}} & 0 & Y_{\delta_{ped}} \\ 0 & 0 & Z_{\delta_{col}} & 0 \\ 0 & L_{\delta_{lat}} & 0 & L_{\delta_{ped}} \\ M_{\delta_{long}} & 0 & 0 & 0 \\ 0 & N_{\delta_{lat}} & 0 & N_{\delta_{ped}} \\ 0 & 0 & 0 & 0 \\ 0 & 0 & 0 & 0 \\ 0 & 0 & 0 & 0 \end{bmatrix} \quad (20)$$

Since Eq. (19) and Eq. (20) are nearly decoupled, the flying quality level of interaxis coupling of the helicopter may reach level 1 now, and this can be proven by Fig. 3 ~ Fig. 6. However, the other flying quality requirements such as stability, control bandwidth etc. are still not improved. Therefore, ideal poles should be designed according to these flying quality requirements. In this paper, the ideal poles in hover and low speed flight states are designed based on small-amplitude attitude change (short-term and mid-term responses to control inputs) and response to collective controller. In forward flight state, besides the above requirements, lateral-directional stability is also considered in ideal poles design.

The ideal poles in longitudinal channel include 1 negative real pole and 2 conjugate complex poles. The negative real pole represents longitudinal damping, and the complex poles represent longitudinal dynamic mode of a helicopter, such as hover oscillation or phugoid in forward flight. The values of ideal poles can be determined by numeric optimization method. The original longitudinal damping of a helicopter can be used as initial value of negative real pole, initial guess of complex poles can be determined easily according to Fig. 14 by selecting an arbitrary point in Level 1 area. Then these poles can be optimized by newton algorithm to ensure the bandwidth of a helicopter reaches desired Level 1 value according to ADS-33E-PRF.

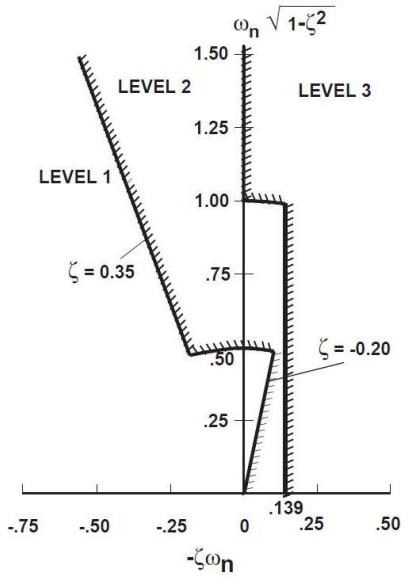

Figure 14: Limits on pitch (roll) oscillations in hover and low speed.

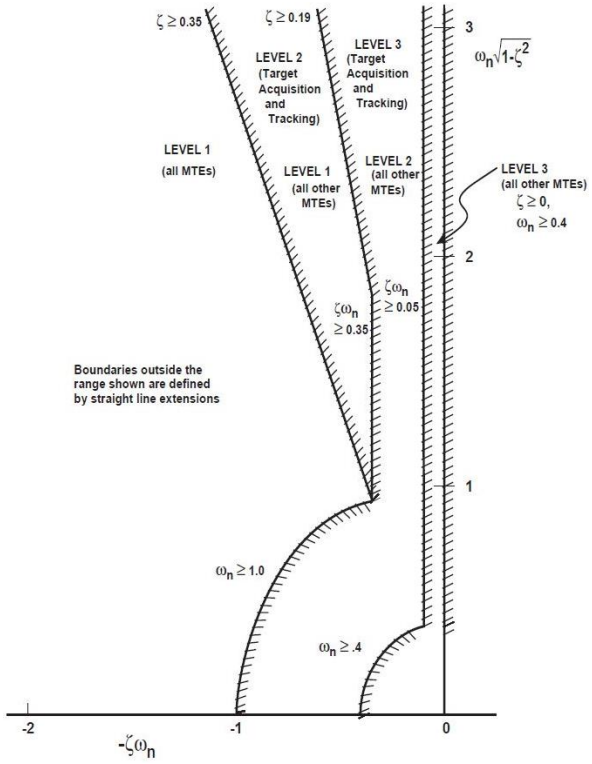

Figure 15: Lateral-directional oscillatory requirements.

The ideal poles in lateral-directional channel include 3 negative real poles and 2 conjugate complex poles. The negative real poles represent lateral damping, yaw damping and spiral mode, and the complex poles represent lateral hover oscillation or Dutch roll mode in forward flight. The values of lateral ideal poles can be determined using the same method as in longitudinal channel. Initial guess of complex poles can be determined according to Fig. 14 in hover and low speed flight and Fig. 15 in forward flight state.

Vertical idea pole can be set based on height response characteristics requirement. In ADS-33E-PRF, this requirement only need vertical rate response have a qualitative first-order appearance for at least 5 seconds following a step collective input. Therefore, vertical ideal pole can be set as a proper negative real number directly.

When all the ideal poles are determined, the next step is to solve the pole placement problem, as defined in Eq. (21). A sufficient and necessary condition for Eq. (21) has a solution is (***A***, ***B***) is fully controllable. It is obviously that all state variables of a helicopter can be controlled by pilot, i.e. (***A***, ***B***) is fully controllable. There are many comprehensive solvers to calculate the feedback control matrix $\boldsymbol{K}_{pole}$. In this paper, the same algorithm as "place" function in MATLAB software is used to obtain a solution of Eq. (21).

$$\lambda_i(\boldsymbol{A}-\boldsymbol{B}\boldsymbol{K}_{pole})=\lambda_i^*,\quad i=1,2,\cdots,n \tag{21}$$

The closed-loop poles in Eq. (21) will be exactly the same value as desired ideal poles. Moreover, if the open-loop poles of ***A*** matrix in Eq. (21) have small changes, the closed-loop poles will be very close to the desired ideal poles by using the same feedback matrix $\boldsymbol{K}_{pole}$. This indicates the performance of the controller will maintain well by using one constant $\boldsymbol{K}_{pole}$ matrix in a reasonable flight state range. Therefore, there is no need to do pole placement calculation at each sampling time. In this paper, an adaptive strategy for pole placement is developed which can be illustrated by Fig. 16. In each sampling time, the open-loop eigenvalues of matrix ***A*** in Eq. (19) are calculated. Then these eigenvalues will be compared with baseline eigenvalues. If the relative variation of any eigenvalues is greater than 10%, the value of cost function *J* will be 1. Otherwise, the cost function *J* will be -1. If the cost function has a positive value, then the pole placement is carried out, and the baseline eigenvalues will be replaced by current open-loop eigenvalues. On the contrary, if the cost function has a negative value, no calculation and no update are required. The baseline eigenvalues can be initialized by a zero vector, and then the pole placement will surely be carried out at the first sampling point.

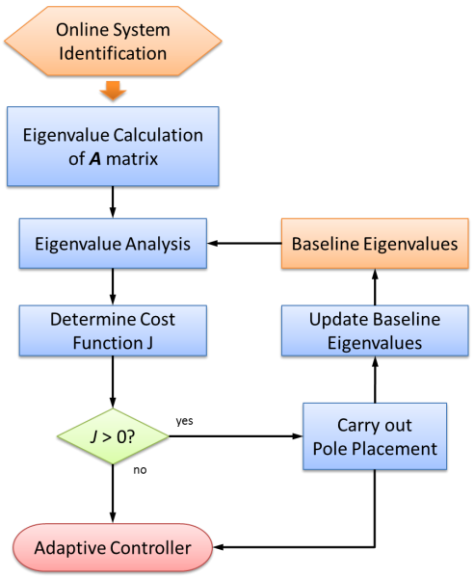

Figure 16: Adaptive Pole Placement Strategy.

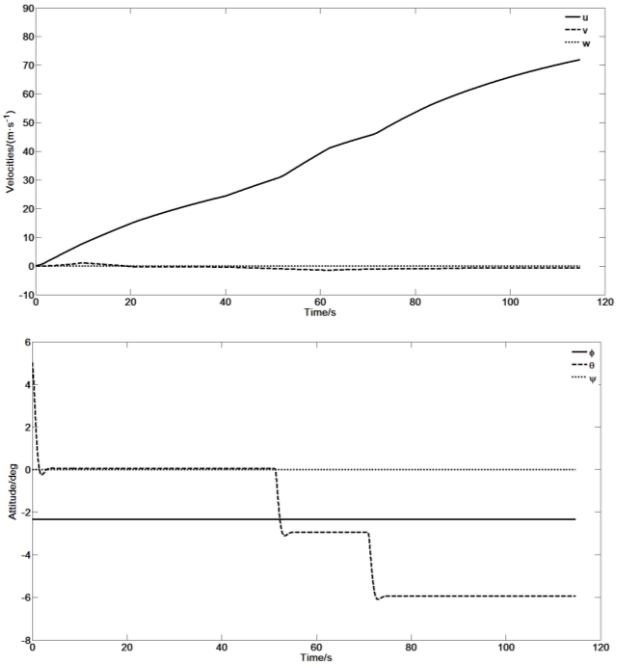

Figure 17: Verification of ACAH response types.

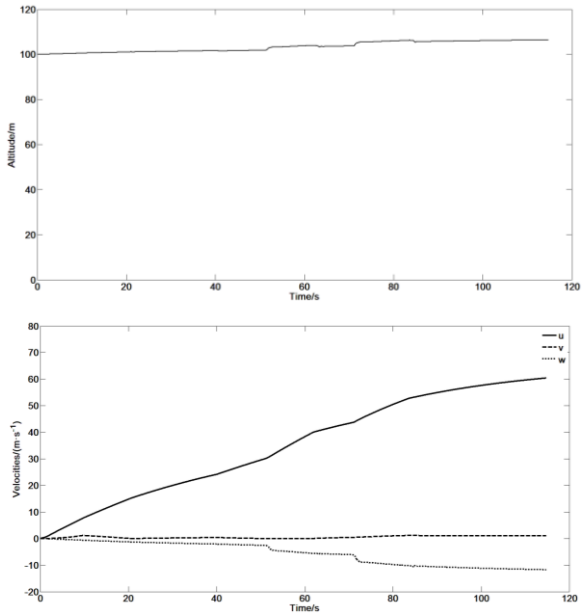

Figure 18: Verification of HH response types.

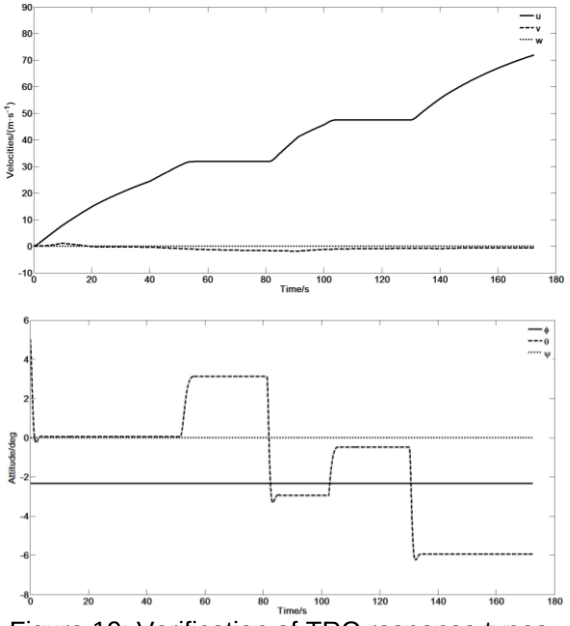

Figure 19: Verification of TRC response types.

Based on the developed adaptive pole placement controller, Attitude Command Attitude Hold (ACAH), Height Hold (HH) and Translational Rate Command (TRC) response types defined in ADS-33E-PRF are implemented for a UH-60 helicopter. Fig. 17 ~ Fig. 19 shows the verification of these 3 response types. It can be found that all 3 response types meet the requirements in flying quality specification. Moreover, the performance of the controller is maintained well from hover to high speed forward flight state. This indicates the adaptive control law designed in this paper is effectiveness.

6. CONCLUSIONS

A comprehensive adaptive flight controller design method for improving helicopter flying quality is developed in this paper. Main achievements and improvements can be summarized as follows:

1) An inner-loop decoupling controller based on dynamic inversion technique is very useful to decrease the difficulties in designing outer-loop adaptive controller. Weak coupled model has very simple model structure, which is very helpful to increase the efficiency in online system identification and pole placement calculation.

2) An improved online system identification method is developed. The introduction of noise model helps to solve the biased estimation problem caused by colored measurement noise, so that the overall identification accuracy is increased. The established recursive extended least squares algorithm with a fixed length window is proven to be very effective and efficient in real time system identification of helicopter flight dynamics model.

3) Outer-loop adaptive controller is designed based on real time pole placement algorithm. It is very convenient to use such controller to improve flying quality since many flying quality requirements can be represented by ideal poles. The adaptive strategy based on eigenvalue analysis is easy to implement. This adaptive rule eliminates all unnecessary adjustments of feedback control matrix, which helps to increase the stability and efficiency of the adaptive controller.

7. ACKNOWLEDGMENTS

This work was co-supported by the National Natural Science Foundation of China (No. 61503183) and the Aeronautical Science Foundation of China (No. 2015ZA52002).

8. REFERENCES

[1] David G. Mitchell, David B. Doman, David L. Key, David H. Klyde, David B. Legget, David J. Moorhouse et al, " Evolution, Revolution, and Challenges of Handling Qualities, " Journal of Guidance, Control and Dynamics; Vol. 27, No. 1, 2004, pp. 12-28.

[2] Aeronautical Design Standard, Handling Qualities Requirements for Military Rotorcraft. U.S. Army Aviation and Missile Command, Redstone Arsenal, AL; 2000. Standard No.: ADS-33E-PRF.

[3] Robert T.N. Chen, William S. Hindson, "Analytical and Flight Investigation of the Influence of Rotor and Other High-Order Dynamics on Helicopter Flight-Control System Bandwidth," NASA -TM-86696, 1985.

[4] C. Fielding, P. K. Flux, "Non-linearities in flight control systems," The Aeronautical Journal, 2003, pp. 673-696.

[5] K. H. Landis, S. I. Glusman, "Development of ADOCS controllers and control laws. Volume 1- Executive summary," NASA CR-177339, 1985.

[6] Chad R. Frost, William S. Hindson, Ernesto Moralez, George E. Tucker, James B. Dryfoos, "Design and Testing of Flight Control Laws on The RASCAL Research Helicopter," AIAA Modeling and Simulation Technologies Conference and Exhibit, Monterey, California, 2002.

[7] Mark B. Tischler, Christopher L. Blanken, Kenny K. Cheung, Sean S. M. Swei et al, "Modernized Control Laws for UH-60 BLACK HAWK Optimization and Flight-Test Results," Journal of Guidance, Control and Dynamics, Vol. 28, No. 5, 2005, pp. 964-978.

[8] Peter J. Gorder, Ronald A. Hess, "Robust Rotorcraft flight Control System Design Including Rotor Degrees of Freedom," AIAA Guidance, Navigation, and Control Conference, Scottsdale, AZ, U.S.A, 1994.

[9] J. Gadewadikar, F.L Lewis, Kamesh Subbarao, Kemao Peng, Ben Chen, "H-Infinity Static Output-Feedback Control for Rotorcraft," AIAA Guidance, Navigation, and Control Conference and Exhibit, Keystone, Colorado, 2006.

[10] S. Suresh, S. N. Omkar, V. Mani, N. Sundararajan, "Nonlinear Adaptive Neural Controller for Unstable Aircraft," Journal of Guidance, Control and Dynamics, Vol. 28, No. 6, 2005, pp. 1103-1111.

[11] Zheng Qu, Anuradha M. Annaswamy, "Adaptive Output-Feedback Control with Closed-Loop Reference Models for Very Flexible Aircraft," Journal of Guidance, Control and Dynamics, Vol. 39, No. 4, 2016, pp. 873-888.

[12] S. Suresh, N. Sundararajan, P. Saratchandran, “Neural Adaptive Flight Controllers for Helicopters,” 44th AIAA Aerospace Sciences Meeting and Exhibit, Reno, Nevada, 2006.

[13] Keng Peng Tee, Shuzhi Sam Ge, Francis E. H. Tay, “Adaptive Neural Network Control for Helicopters in Vertical Flight,” IEEE Transactions on Control Systems Technology, Vol. 16, No. 4, 2008, pp. 753-762.

[14] Nathan D. Richards, Richard J. Adams, David H. Klyde, Bruce Cogan, “Flight-Test Evaluation of an Adaptive Controller for Flying Qualities Specification and Protection,” Journal of Guidance, Control and Dynamics, Vol. 38, No. 12, 2015, pp. 2241-2256.

[15] Geethalakshmi S. Lakshmikanth, Radhakant Padhi, John M. Watkins, James E. Steck, “Adaptive Flight-Control Design Using Neural-Network-Aided Optimal Nonlinear Dynamic Inversion,” Journal of Aerospace Information Systems, Vol. 11, No. 11, 2014, pp. 785-806.

[16] Vahram Stepanyan, Kalmanje Krishnakumar, “Adaptive Control with Reference Model Modification,” Journal of Guidance, Control and Dynamics, Vol. 35, No. 4, 2012, pp. 1370-1374.

[17] L. Hoecht, T. Bierling, F. Holzapfel, “Ultimate Boundedness Theorem for Model Reference Adaptive Control Systems,” Journal of Guidance, Control and Dynamics, Vol. 37, No. 5, 2014, pp. 1595-1603.

[18] J. Grauer, J. Conroy, J. Humbert, D. Pines, “System Identification of a Miniature Helicopter,” Journal of Aircraft, Vol. 46, No. 4, 2009, pp. 1260-1269.

[19] M. Elshafei, S. Akhtar, M. S. Ahamed, “Parametric Models for Helicopter Identification Using ANN,” IEEE Transactions on Aerospace and Electronic Systems, Vol. 36, No. 4, 2000, pp. 1242-1252.

[20] Ravindra Jategaonkar, Dietrich Fischenberg, Wolfgang von Gruenhagen, “Aerodynamic Modeling and System Identification from Flight Data—Recent Applications at DLR,” Journal of Aircraft, Vol. 41, No. 4, 2004, pp. 681-691.

[21] Tischler, M., Remple, R., Aircraft and Rotorcraft System Identification: Engineering Methods with Flight test Examples 2nd Edition, AIAA Education Series, AIAA, Reston, VA, 2012, pp. 1-20.

[22] Wu Wei, Chen Renliang, “Set-Membership Identification Method for Helicopter Flight Dynamics Modeling,” Journal of Aircraft, Vol. 52, No. 2, 2015, pp. 553-560.

[23] Li Pan, Chen Renliang, “A mathematical model for helicopter comprehensive analysis,” Chinese Journal of Aeronautics, Vol. 23, No. 3, 2010, pp. 320-326.